
A MATRIX VARIATIONAL AUTO-ENCODER FOR VARIANT EFFECT PREDICTION IN PHARMACOGENES

Antoine Honoré^{1*}, Borja Rodríguez Gálvez³, Yoomi Park², Yitian Zhou²,
Volker M. Lauschke², Ming Xiao¹

¹ Division of Information Science and Engineering, KTH, Stockholm, Sweden

² Department of Physiology and Pharmacology, Karolinska Institutet, Stockholm, Sweden

³ Independent researcher

ABSTRACT

Variant effect predictors (VEPs) aim to assess the functional impact of protein variants, traditionally relying on multiple sequence alignments (MSAs). This approach assumes that naturally occurring variants are fit, an assumption challenged by pharmacogenomics, where some pharmacogenes experience low evolutionary pressure. Deep mutational scanning (DMS) datasets provide an alternative by offering quantitative fitness scores for variants. In this work, we propose a transformer-based matrix variational auto-encoder (matVAE) with a structured prior and evaluate its performance on 33 DMS datasets corresponding to 26 drug target and ADME proteins from the ProteinGym benchmark. Our model trained on MSAs (matVAE-MSA) outperforms the state-of-the-art DeepSequence model in zero-shot prediction on DMS datasets, despite using an order of magnitude fewer parameters and requiring less computation at inference time. We also compare matVAE-MSA to matENC-DMS, a model of similar capacity trained on DMS data, and find that the latter performs better on supervised prediction tasks. Additionally, incorporating AlphaFold-generated structures into our transformer model further improves performance, achieving results comparable to DeepSequence trained on MSAs and finetuned on DMS. These findings highlight the potential of DMS datasets to replace MSAs without significant loss in predictive performance, motivating further development of DMS datasets and exploration of their relationships to enhance variant effect prediction.

1 INTRODUCTION

Variant effect predictors (VEPs) are mathematical models aiming at predicting the effect of one or multiple variants in a sequence of amino-acids (AAs). The effect of a protein variant is typically defined as a loss or gain of function of a cell carrying the variant, compared to a cell carrying a wild-type (WT) protein without variant. The accurate prediction of variant effect has many promising applications for personalized medicine, particularly in the field of pharmacogenomics, where variants on drug targets or Absorption-Distribution-Metabolism-Excretion (ADME) proteins are of particular interest (Huang et al., 2016). In this context, VEPs can be used to assess individual patient response to chemotherapeutic treatments from their genetic background, thus eliminating the need for multiple attempts at treatments. The most effective VEPs have been designed using data from multiple sequence alignments (MSAs) and based on the *conservation assumption*: fit variants are selected out by nature and thus, learning a distribution over variants found in nature implicitly captures the biochemical constraints that characterize fit variants. New sequencing techniques combined with machine learning could lead to significant advances in variant effect prediction, by providing quantitative data in region of the protein sequence space unexplored in existing MSA datasets. Deep mutational scanning (DMS) has recently emerged as a way to yield large-scale datasets of protein

*Corresponding author: antoinehonor@gmail.com. This work was partially supported by the Wallenberg AI, Autonomous Systems and Software Program (WASP) funded by the Knut and Alice Wallenberg Foundation. The computations were enabled by the Berzelius resource provided by the Knut and Alice Wallenberg Foundation at the National Supercomputer Centre.

quantitative fitness scores (Fowler & Fields, 2014). The fitness scores can also be obtained with different selection assays, allowing to quantify various effects, e.g. effect on phenotype or effect on structure. DMS thus allows to challenge the conservation assumption of VEPs design from MSAs. This is in turn is of particular importance in pharmacogenomics, since pharmacogenes are generally under low evolutionary pressure (Zhou et al., 2022; Ingelman-Sundberg et al., 2018).

In this article, we design a VEP and use it to evaluate the validity of the conservation assumption for pharmacogene-related proteins. Our architecture exploits the structure of variational auto-encoders (VAEs) and allows models of similar capacity and designs to be trained on both MSA and DMS data. We also exploit a transformer architecture in order to improve upon existing VAE-based VEPs. Both VAE and transformers are key components of the best performing models in the ProteinGym benchmark (Notin et al., 2023a). We experiment with a VAE-based model exploiting multimodal priors, and we derive a matrix encoding scheme inspired from linear matrix decomposition to replace the input flattening operation found for instance in DeepSequence.

Contributions Our contributions are summarized as follows:

1. We design protein specific models combining a VAE and a transformer for variant effect prediction. We study their zero-shot prediction performances on 33 deep mutational scanning (DMS) datasets of drug related and ADME proteins available in the ProteinGym benchmark.
2. We propose a new way to train VAEs for deep unsupervised clustering using expressive latent prior based on discrete distributions. We evaluate the model on zero-shot predictions when trained on MSA data available in ProteinGym. We experiment with and without adding protein structure information to our model.
3. We adapt our model to directly predict labels from DMS datasets using a prediction head from the latent space, thus preserving our model capacity. In light of the comparison in performances of the models trained unsupervised on MSA and supervised DMS label data, we discuss the extent of the validity of the conservation assumption.

1.1 RELATED WORKS

Zero-shot predictors VEPs exploiting site-independent position-wise frequencies of AAs in MSAs remain the methods of choice in pharmacology, e.g. SIFT or Polyphen-2 (Ng & Henikoff, 2003; Adzhubei et al., 2010; Durbin, 1998). However, other models can achieve much better zero-shot prediction performances on at least one pharmacogene-related protein DMS dataset (Details in Table A.5), according to the recent ProteinGym variant effect prediction benchmark (Notin et al., 2023a). Many of these models compute the functional cellular effect of a variant v compared to a wild-type sequence $\underline{x}^{(wt)}$, via the log-likelihood ratio:

$$\hat{y} = \ln \frac{p(\underline{x}^{(v)})}{p(\underline{x}^{(wt)})}, \quad (1)$$

where $p(\cdot)$ is a generative probability density chosen to maximize $p(\underline{x}^{(v)})$, for sequences $\underline{x}^{(v)}$ from the MSA. For instance, the Evolutionary Scale modeling (ESM) approaches (Rives et al., 2021), rely solely on a transformer-based protein language model (PLM) for modeling the distribution over sequences in MSAs. Tranception (Notin et al., 2022a) additionally integrates predictions using position-wise frequencies of AAs in MSAs. TranceptEVE (Notin et al., 2022b) combines the Tranception model with a VAE-based model (Frazer et al., 2021) for AA sequence modeling. Other methods such as Masked Inverse Folding (MIF) (Yang et al., 2023) learn to predict protein sequences from a given structure. VESPA (Marquet et al., 2022) combines protein sequence embedding from PLMs with known bio-mechanical properties of AAs to predict variant effect with a linear regression model. Other model do not rely on the ratio in (1) to compute variant effect. MSA Transformer (Rao et al., 2021) is based on ESM and uses axial attention to optimize a masking loss over an entire MSA, rather than on individual sequences. It learns a representation of Hamming distances in the MSA and the hamming distance to WT sequence is used as a proxy for variant effect. GEMME (Laine et al., 2019) predicts variant effect via the distance to WT sequence in an evolutionary tree. This approach shows very good performances and has several order of magnitude fewer parameters than transformer-based approaches. DeepSequence (Riesselman et al., 2018) introduces a VAE and approximates the distribution of input data \underline{x} (Eq. (1)) with the variational evidence lower bound.

Supervised learning predictors Recently, several models combining DMS and MSA datasets have been proposed Hsu et al. (2022). The general idea is to combine sequence embeddings, e.g. sequence one-hot encoding, with evolutionary fitness scores from pretrained models such as ESM or DeepSequence. ProteinNPT is a conditional pseudo-generative model designed for exploiting DMS data, jointly with MSA data in a semi-supervised framework (Notin et al., 2023b). In addition to their novel architecture, the authors introduce several baselines consisting in exploiting prediction scores from zero-shot prediction models pretrained on MSA, including DeepSequence and MSA Transformer. SPIRED is a recent framework able to predict fitness scores as well as protein structure (Chen et al., 2024). A pretrained ESM model is used for sequence embedding, and graph attention networks and multilayer perceptron are trained using DMS data in a supervised framework.

Multi-modal prior distributions for VAEs VAEs, e.g. DeepSequence, assume that the input data $\underline{\mathbf{x}} \in \{0, 1\}^{L \times d}$ are generated from a latent variable of a D -dimensional vector space: $\mathbf{z} \in \mathbb{R}^D$. The latent variable is assumed drawn from a Gaussian prior $p(\mathbf{z})$, and the generative process is modeled with a distribution $p_{\theta}(\underline{\mathbf{x}}|\mathbf{z})$. The explicit modeling of the latent variable \mathbf{z} is an interesting feature of VAEs, because it allows to put a formal prior distribution on the latent space. The other mentioned models do not impose such structure, although interestingly the learnt representations in ESM was shown to correlate with known bio-mechanical properties of AAs (Rives et al., 2021). Multimodal mixture of Gaussian (MOG) priors have been proposed as latent prior distributions for unsupervised clustering tasks (Dilokthanakul et al., 2017) with VAE. The authors used trainable mean and covariances in latent space and showed through data sampling that the learnt mixture components corresponded to meaningful characteristics of the input data. This was shown to have potential implications for model interpretability in biological contexts (Varolgüneş et al., 2020). Further, the VampPrior has been designed so that the statistics of the mixture components explicitly depend on input space prototypes Tomczak & Welling (2018). This provides meaningful variables to probe for interpretability rather than using a sampling scheme. Bayesian VAEs such as DeepSequence were shown to have good performances as VEP. However, they require a lot of parameters (30M) and a lot sampling in order to get good results. This makes them difficult to use as expert model in an ensemble for instance. To the best of the authors knowledge, current methods employing VAEs for VEP have only been designed with unimodal prior distributions. We propose to structure the latent with an implicit mixture of discrete distributions, which is readily interpretable, reduces the number of parameters, and does not require sampling at inference.

2 METHODS

A detailed description of the matVAE-MSA architecture is provided in section 2.1. A reduction of the architecture with similar capacity and that can be trained on DMS data: matENC-DMS, is proposed in section 2.2. The datasets that are used to train and evaluate the models are introduced in section A.2.

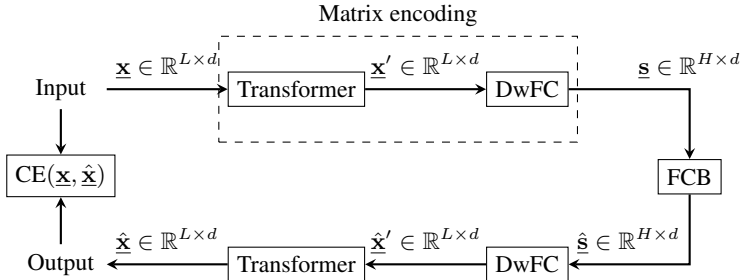


Figure 1: Model architecture of matVAE-MSA. DwFC: Dimensionwise fully connected layer. CE: Cross-entropy loss. FCB: Fully connected bottleneck.

2.1 MODEL DESCRIPTION

2.1.1 MATRIX DECOMPOSITION AND ENCODING

Matrix decomposition is a set of methods in linear algebra consisting in decomposing a matrix $\underline{\mathbf{x}} \in \mathbb{R}^{L \times d}$ (here $d < L$), into two (or more) matrices with interesting structure, e.g. unitary, triangular, diagonal. For instance, the QR decomposition of $\underline{\mathbf{x}} \in \mathbb{R}^{L \times d}$ is of the form $\underline{\mathbf{x}} = \mathbf{Q}[\mathbf{R}^T, \mathbf{0}^T]^T$, where $\mathbf{Q} \in \mathbb{R}^{L \times L}$ is unitary, $\mathbf{R} \in \mathbb{R}^{d \times d}$ is upper triangular and $\mathbf{0}$ is a $(L - d \times d)$ -dimensional matrix of zeros. We call matrix encoding the use of the low dimension factor, here the \mathbf{R} matrix, as a compressed representation of the input $\underline{\mathbf{x}}$. For QR decomposition, the matrix encoding can be formulated:

$$[\underline{\mathbf{s}}^T, \mathbf{0}^T]^T = \mathbf{W}\underline{\mathbf{x}} \in \mathbb{R}^{L \times d}, \quad (2)$$

where $\mathbf{W} = \mathbf{Q}^{-1} \in \mathbb{R}^{L \times L}$ is a linear transform and $\underline{\mathbf{s}} = \mathbf{R}$. Linear decomposition methods are often related to singular value decomposition, for instance the diagonal elements of \mathbf{R} in the QR decomposition are the singular values of $\underline{\mathbf{x}}$. However, for one-hot encoded sequences of AAs, the singular values are counts of each AA in the sequence, and the singular vectors are a permutation of \mathbb{I}_d determined by the ordering of the counts of the AAs. In other words, the encoding produced with such linear methods does not account for the global or relative position of AAs in the sequence, and in particular, randomly permuting the rows of $\underline{\mathbf{x}}$ leads to the same encoding. To ensure that the model is flexible enough to learn a useful encoding, we propose to learn a representation of $\underline{\mathbf{x}}$ with a transformer, prior to reducing the first dimension to a fixed $H < L$ with a trainable linear transform. This is formulated as follows:

$$\begin{aligned} \underline{\mathbf{x}}' &= \text{Transformer}(\underline{\mathbf{x}}) \in \mathbb{R}^{L \times d}, \\ \underline{\mathbf{s}} &= \text{DwFC}(\underline{\mathbf{x}}') \in \mathbb{R}^{H \times d}, \end{aligned}$$

where $\text{Transformer}(\cdot)$ and $\text{DwFC}(\cdot)$ are specified in the paragraphs below.

Transformer Transformers are effective sequence models that can transfer information between any two positions within a sequence. The model we use is similar to the multi-layer encoding transformer in (Vaswani et al., 2017). Individual layers encode an input sequence $\underline{\mathbf{x}} \in \mathbb{R}^{L \times d}$ into a sequence $\underline{\mathbf{x}}' \in \mathbb{R}^{L \times d}$ as follows:

$$\begin{aligned} \underline{\mathbf{x}}_1 &= \text{Norm}(\tau_1 \underline{\mathbf{x}} + (1 - \tau_1) \text{Attn}(\underline{\mathbf{x}})), \\ \underline{\mathbf{x}}' &= \text{Norm}(\tau' \underline{\mathbf{x}}_1 + (1 - \tau') \text{FC}(\underline{\mathbf{x}}_1)), \end{aligned} \quad (3)$$

where $\text{Norm}(\cdot)$ is a Layer Normalization (Ba et al., 2016), $\text{FC}(\cdot)$ is a fully connected (FC) network with ReLU activations, and $\text{Attn}(\cdot)$ is the masked scaled dot product attention from (Vaswani et al., 2017). We use trainable $\tau_1, \tau' \in [0, 1]^2$ to control the gradient flow in the gated skip connections (He et al., 2016). Note that we do not use positional encoding since (Rives et al., 2021) showed that PLMs did not necessarily benefit from it. Instead, structure information is encoded in the mask of the attention layer (See section A.3).

Dimension-wise FC (DwFC) We call DwFC the FC linear layer inspired from Eq. 2. This layer is similar to a flattening followed by a linear transform with bias, but requires less parameters since the same linear transform is used across dimensions. This operation replaces the direct flattening of the input in DeepSequence. $\underline{\mathbf{x}}' \in \mathbb{R}^{L \times d}$ is encoded in a protein length independent representation $\underline{\mathbf{s}} \in \mathbb{R}^{H \times d}$ as follows:

$$\underline{\mathbf{s}} = \mathbf{U}\underline{\mathbf{x}}' + \mathbf{b}, \quad (4)$$

where $\mathbf{U} \in \mathbb{R}^{H \times L}$ and $\mathbf{b} \in \mathbb{R}^H$ are trainable weight and bias parameters.

2.1.2 FULLY CONNECTED BOTTLENECK (FCB) WITH DIRICHLET LATENT PRIOR

We extend the work carried out in DeepSequence, by using the simplex $S^D = \{\mathbf{z} \in [0, 1]^D \mid \sum_i z_i = 1\}$ as latent space. The FCB is similar to a classical VAE (Kingma & Welling, 2014). The input $\underline{\mathbf{s}} \in \mathbb{R}^{H \times d}$ is flattened and then encoded into a latent representation of fixed dimension:

$$\mathbf{h} = \text{softmax}(\text{FC}(\text{Vec}(\underline{\mathbf{s}}))) \in \mathbb{R}^D, \quad (5)$$

where $\text{Vec}(\cdot)$ denotes the flattening operation and $\text{softmax}(\cdot)$ ensures that the vector \mathbf{h} represents a discrete probability distribution. For training, we introduce robustness by drawing the latent vector $\mathbf{z} \sim \text{GumbelSoftmax}(\mathbf{h})$ using the reparameterization trick (Potapczynski et al., 2020). At test time, we use $\mathbf{z} = \mathbf{h}$ to reduce stochasticity. The latent vector $\mathbf{z} \in \mathbb{R}^D$ is then used as input to a decoder network that aims to reconstruct the input $\underline{\mathbf{s}}$. The output to the decoding part of the FCB, is denoted $\hat{\underline{\mathbf{s}}} \in \mathbb{R}^{H \times d}$.

2.1.3 DECODING

The decoding process denoted $p_\theta(\underline{\mathbf{x}}|\mathbf{z})$, is symmetrical to the encoder, i.e. consists of a decoding FC layer, and a dimension wise FC layer followed by a transformer. One important difference is that the decoding transformer includes a temperature softmax output operation to ensure that the rows of the reconstructed $\hat{\underline{\mathbf{x}}} \in \mathbb{R}^{L \times d}$ define proper discrete distributions.

2.1.4 LOSS FUNCTION

Our loss function is directly derived from the negative evidence lower bound (ELBO) used in VAEs (Kingma & Welling, 2014):

$$\text{ELBO}(\underline{\mathbf{x}}; \phi, \theta) = D_{KL}(q_\phi(\mathbf{z}|\underline{\mathbf{x}})||p(\mathbf{z})) + \mathbb{E}_{q_\phi}[\log p_\theta(\underline{\mathbf{x}}|\mathbf{z})], \quad (6)$$

where on the RHS, the first term is the KLD between the approximated posterior distribution q_ϕ , and the prior p , and the other is an expected reconstruction loss (defined in section A.4).

Prior: Our prior distribution is a mixture of D degenerate discrete distributions described by one-hot vectors. However, KL divergence with a mixture distributions does not exist in closed form. Therefore, formulating it explicitly would require to use a bound instead. In addition it would require specifying or learning statistics of the mixture. Instead, we replace the explicit KL divergence minimization in Eq. (6), with the minimization of the entropy of $\mathbf{h} \in S^D$, $S(\mathbf{h}) = -\sum_i h_i \log h_i$. Intuitively, vectors in S^D with small entropy are close to one hot encoded vectors, and thus minimizing their entropy at training time is equivalent to minimizing the KL divergence between \mathbf{h} and one of the D discrete degenerate distributions (Proof in A.1). Our loss function is written as follows:

$$l(\underline{\mathbf{x}}; \theta, \phi) = - \left(-\beta \sum_i h_i \log h_i + \mathbb{E}_{q_\phi(\mathbf{z}|\underline{\mathbf{x}})} [\ln p_\theta(\underline{\mathbf{x}}|\mathbf{z})] \right), \quad (7)$$

where $\beta > 0$ is a tunable parameter and $\mathbf{h} = q_\phi(\mathbf{z}|\underline{\mathbf{x}})$ (Eq. (5)). Our approach has several advantages over a classical mixture of Gaussian: First, we do not need to specify/learn prior statistics except for the maximum number of components ($=D$). For MoG, components weight, mean and standard deviation must be specified or learnt. This reduces the number of trainable parameters and/or avoids certain inductive biases on the prior. Second, this leads to a structured latent space with latent vectors directly interpretable as class probabilities, which is ideal for deep unsupervised clustering problems. Third, the prior is never explicitly formulated as a mixture which would require computing a bound on the KL divergence, instead we use the entropy of the vectors that is easy to compute.

The complete encoding/decoding structure of the model depicted in Fig. 1 is trained on MSA data to minimize (7). At test time, the loss in (7) is used with $\beta = 1$ as an approximation of the log-evidence in order to compute the log-likelihood ratio in (1).

2.2 REDUCTION OF THE MODEL FOR DMS DATA

Our reduced model uses the encoding part of matVAE-MSA, and replaces the decoding part with a FC network prediction head to predict the quantitative DMS score $y \in \mathbb{R}$:

$$\begin{aligned} \mathbf{h} &= \text{Softmax}(\text{FC}(\text{Vec}(\text{DwFC}(\text{Transformer}(\underline{\mathbf{x}})))))) \in \mathbb{R}^D, \\ \hat{y} &= \text{FC}(\mathbf{h}) \in \mathbb{R}, \end{aligned}$$

where $\mathbf{h} \in \mathbb{R}^D$ is similar to (5). The reduced model depicted in Fig. 2 is referred to as ‘‘matENC-DMS’’. matENC-DMS has a capacity very close to that of matVAE-MSA since the encoder is identical in the two models, and the decoder of matVAE-MSA is symmetrical to the encoder and only aims at reconstructing the input. We argue that this is an ideal setup to test the conservation assumption often used when designing VEPs: unfit variants were selected out by nature and thus, learning

a distribution over these sequences implicitly captures the biochemical constraints that characterize fit variants.

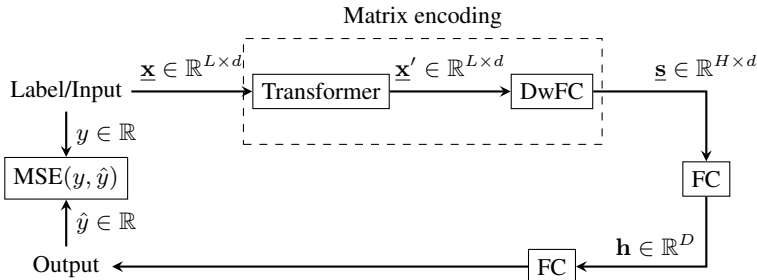


Figure 2: Model architecture of matENC-DMS. DwFC: Dimensionwise fully connected layer. CE: Cross-entropy loss. FC: Fully connected.

3 EXPERIMENTS

In this section we provide details on our experimental design choices. Our model comparison setup with the choice of baselines and performance metrics is explained in 3.1. The model architecture and training hyper-parameters are discussed in A.3 and A.4. The code is available: <https://github.com/antoinehonore/matVAE>.

3.1 MODEL COMPARISON

Performance metrics The performances of our protein specific models are measured and reported on corresponding individual DMS datasets, both in terms of Spearman’s Rank Correlation coefficient (SpearmanR) and area under receiver operating characteristic (AUROC). The SpearmanR measures the correlation between the ranks of the predicted scores and the ranks of the target scores. Additionally, the target score is binarized in order to compute the AUROC. To allow for a meaningful comparison of the AUROC scores, we use the binarization threshold used in ProteinGym. In brief, given a DMS dataset, a threshold on the scores is selected manually between modes in case the distribution of scores is bimodal, and as the median in case the distribution of scores is unimodal. In the rest of the paper we will primarily compare spearmanR performances.

For matENC-DMS, we train our model on DMS data with supervised learning in a 5-fold cross-validation framework. Firstly, this ensures that no variant/label pair is used for both training and testing. Secondly, this ensures that the evaluation framework is comparable to that of matVAE-MSA, with all variants in the DMS dataset used exactly once for validation. When a protein has multiple DMS datasets, we performed separate cross-validations on each dataset. The performances on individual DMS datasets are then reported as the average of the 5 models trained on independent training sets.

Model design and training We experimented with models of various latent space sizes and found that $D = 10$ had best performances for MSA training. We kept this dimension for the rest of the experiments. We also experimented with and without the use of the AlphaFold structures, i.e. with and without the Transformer(.) layer, as well as training matENC-DMS on DMS data only, and finetuning matVAE-MSA with DMS data (matENC-FT).

Baselines All models with zero-shot prediction performances reported in the ProteinGym benchmark were considered for inclusion as a baseline. Only those models that demonstrated the highest SpearmanR zero-shot performances on at least one pharmacogene-related protein DMS dataset were used as a baseline. These models fall into one of the following model families: DeepSequence (Rieselman et al., 2018), ESM (Rives et al., 2021), Tranception (Notin et al., 2022a), MIF (Laine et al., 2019), GEMME (Laine et al., 2019), VESPA (Marquet et al., 2022), MSA Transformer (Rao et al., 2021). Within each family, the top-performing models vary in configuration (e.g., different parameter counts), which we refer to as model "flavors" (See Table A.5). For example ESM2 (150M),

Source	Model Name	Short Description
Our experiments	matVAE-MSA	Matrix variational auto-encoder trained on MSA data (Fig. 1)
	matVAE-MSA +AF	matVAE-MSA with the use of AF structures
	matENC-DMS	Matrix encoder trained on DMS data (Fig. 2)
	matENC-DMS + AF	matENC-DMS using AF structures trained on DMS data
	matENC-FT	matENC-DMS trained on MSA, and fine-tuned on DMS data
	matENC-FT + AF	matENC-DMS using AF structures, trained on MSA and fine-tuned on DMS data
ProteinGym	“Best Benchmark”	Best performing model flavor on a given DMS dataset
	DeepSequence	VAE-based model
	ESM	PLM-based model
	Tranception	PLM and position-wise AA frequency-based model
	TranceptEVE	PLM, EVE and position-wise AA frequency-based model
	MSA Transformer	Position-wise transformer and PLM-based model
	GEMME	Evolutionary tree based model
	VESPA	Linear Ensemble of PLM, bio-mechanic features and position-wise frequency models.
	MIF	PLM and inverse folding model
	Site-Independent	Position-wise entropy-based model

Table 1: Summary of baselines and experiments. AF stands for precomputed AlphaFold structures provided in the ProteinGym benchmark.

ESM2 (15B) and ESM-1v (ensemble) are all distinct flavors within the ESM family. We report the performances at the level of model families, by the average performances of the best performing model flavors of that family on individual DMS datasets. The details of which model flavor performs best on which DMS dataset are shown in Table A.4. We also compare with the “Site-Independent” model of ProteinGym, which is similar to SIFT and Polyphen-2, both still widely used in pharmacogenomics. In addition, we add a difficult baseline referred to as “Best Benchmark”, which is the best performing model flavor across all model families for each DMS dataset (See Table A.5).

To compare our models trained only on DMS data, we use the supervised learning baselines from ProteinGym with 5 “Random” cross-validation splits. For this case the models belong to the following families: ESM, TranceptEVE, Tranception, DeepSequence, MSA Transformer. To the best of the authors knowledge, all these baselines consist of zero-shot prediction models trained on MSA data, and used pretrained in a supervised learning framework with embeddings of the protein sequence (See (Notin et al., 2023a)). ProteinNPT is a slightly different architecture which jointly trains on MSA and DMS data (Notin et al., 2023b). The details of the best performing model flavors are in Table A.6.

The prediction baseline models are summarized in Table 1.

4 RESULTS & DISCUSSION

The results for our internal experiments of our different architectures and training methods are shown in Table 2c. The results are put into perspectives with average zero-shot prediction benchmark in Table 2a and with the supervised prediction benchmark in Table 2b. The raw results of all models for zero-shot predictions are shown in Figure A.4 in terms of SpearmanR and in terms of AUROC in Figure A.5. Similarly, raw results in terms of SpearmanR for supervised predictions benchmarks are shown in Figure A.6.

4.1 ZERO-SHOT PREDICTION RESULTS

When trained with MSA data only and without use of AF structures, our model (matVAE-MSA) performs better on average than “DeepSequence (single)”, with an order of magnitude fewer parameters and two order of magnitude less computationally expensive inference methods¹ (Table 2a). matVAE-MSA also performs better than MIF which is also a much more complex model. In addition, matVAE-MSA performs similarly to an ensemble of DeepSequence-like architectures, which

¹The authors of DeepSequence suggest averaging ELBO approximations over 500 draws of latent variables (See <https://github.com/debbiemarkslab/DeepSequence/blob/master/examples/MutationEffectPrediction.ipynb>), while we do not use sampling.

shows the improvements brought by our design to existing VAE-based VEPs. The improvement in average performances also occurs in terms of AUROC. We also note that these improvements are without an increase in standard deviations, which shows that our model is as reliable as others when evaluated across pharmacogene-based proteins. Interestingly, matVAE-MSA does not benefit from the introduction of the AF structures via an input transformer model (matVAE-MSA + AF). The average performances decrease slightly and are comparable to MIF and "DeepSequence (single)".

4.2 SUPERVISED PREDICTION RESULTS

We evaluate our architecture in a cross-validation framework when trained using labeled DMS data, either from scratch or following pretraining with MSA data (finetuning matVAE-MSA). First, training with DMS data increases average SpearmanR performances overall, whether or not AF structures are used in the model architecture (Table 2c). However, our finetuning experiments show that our model performs poorly compared to other models, whether or not AF structures are used (Table 2b). Coincidentally, both matENC-FT and matENC-DMS + AF have identical performances, although the raw results show different performances on individual DMS datasets Figure. A.6. When training from scratch on DMS data, the use of AF structure (matENC-DMS + AF) provides a substantial increase in performances compared to matENC-DMS, placing our model marginally above DeepSequence. This is particularly interesting because here the DeepSequence model consists of finetuning experiments after DeepSequence is trained on MSA data. Thus, similar performances are obtained with a simpler model and less training time.

When grouping DMS datasets per protein type, we find no significance in gains or loss of performances across groups (Figure. A.7). When grouping DMS datasets per assay selection type, we find that matVAE-MSA improves performances compared to DeepSequence (single) slightly more for Binding assays (Figure. 3b). Interestingly, assays selecting for protein expression show a slightly more pronounced and consistent increase compared to other selection types (Figure. 3d).

Table 2: Numerical results ($\mu \pm \sigma$) for our models against baselines. The models trained by us are in bold font. AF: Use of AlphaFold structures. * zero-shot prediction performances. † supervised prediction performances.

	spearmanr	auroc	Spearmanr	
Best Benchmark	0.529 ± 0.151	0.794 ± 0.076	Best Benchmark	0.689 ± 0.162
ESM	0.508 ± 0.157	0.78 ± 0.079	ProteinNPT	0.671 ± 0.195
TranceptEVE	0.485 ± 0.167	0.763 ± 0.088	Tranception	0.646 ± 0.173
Tranception	0.478 ± 0.165	0.761 ± 0.086	ESM	0.586 ± 0.153
GEMME	0.461 ± 0.155	0.75 ± 0.085	MSATransformer	0.579 ± 0.17
MSA Transformer	0.452 ± 0.167	0.746 ± 0.089	TranceptEVE	0.536 ± 0.156
VESPA	0.445 ± 0.164	0.745 ± 0.095	One-Hot Encoding	0.528 ± 0.168
EVE	0.441 ± 0.165	0.74 ± 0.088	matENC-DMS + AF	0.507 ± 0.183
DeepSequence (ens.)	0.424 ± 0.152	0.728 ± 0.084	DeepSequence	0.501 ± 0.148
matVAE-MSA	0.423 ± 0.15	0.73 ± 0.08	matENC-FT	0.443 ± 0.187
matVAE-MSA + AF	0.416 ± 0.148	0.727 ± 0.08	matENC-FT + AF	0.443 ± 0.187
MIF	0.415 ± 0.165	0.729 ± 0.083	matENC-DMS	0.443 ± 0.173
DeepSequence (single)	0.412 ± 0.149	0.723 ± 0.083		
Site-Independent	0.39 ± 0.145	0.713 ± 0.078		

(a) Zero-shot prediction performances for matVAE-MSA against baselines. DeepSequence (ens.) refers to an ensemble of DeepSequence models with various architectures.

(b) Supervised prediction performances for matENC-DMS against baselines.

Training Data	SpearmanR	
	No AF	AF
MSA only*	0.423 ± 0.15	0.416 ± 0.148
DMS only†	0.443 ± 0.173	0.507 ± 0.183
MSA + DMS†	0.443 ± 0.187	0.443 ± 0.187

(c) Numerical SpearmanR results on DMS datasets for different training methods. MSA + DMS: Model first trained on MSA data, then finetuned with DMS data.

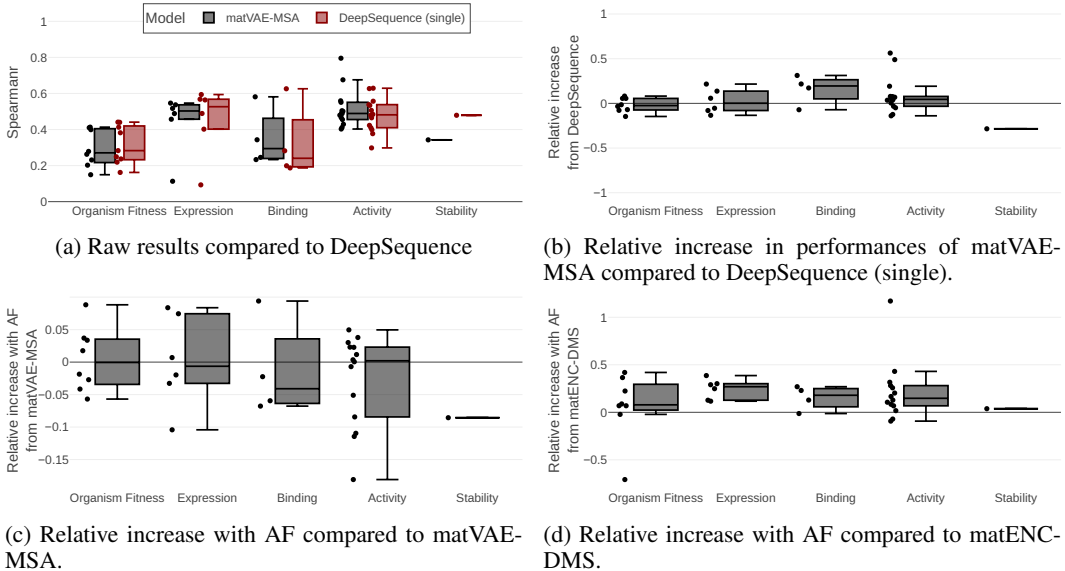


Figure 3: SpearmanR performances of ours models versus other zero-shot prediction models, per Selection Type sub-groups. One point denotes the score obtained on a DMS dataset and the boxplots describe the distribution of scores across DMS datasets.

4.3 FUTURE WORK

Our results experimenting with expressive multi-modal priors did not show improvements compared to simple Gaussian prior. The investigations of the potential pitfalls of our current approach as well as further biology-relevant interpretations of the latent prior modes are left for future works.

Next, the joint use of both DMS and MSA data for training is an important next step towards improved model performances. In our work, our primary objective was to evaluate the information provided by MSA and DMS data separately for variant effect prediction. DMS and MSA data could nonetheless be used jointly for training, for instance in a fine tuning approach, where a VAE model is first trained on MSA data, and the encoding part is fine tuned on DMS data. This might lead to improved performances since both datasets would then contribute to the model performances. Together with experimentation on a wider range of proteins, fine tuning on DMS data is an interesting research direction that we leave as future work.

Lastly, the design of a model able to learn from multiple proteins is also an interesting next avenue for research. Our current architecture can be extended to work for proteins of different lengths L_1, L_2, \dots . This could be done by slightly modifying the DwFC layer (Eq. (4)). An idea would be to first define $L_M = \max(L_1, L_2, \dots)$ and initialize $\mathbf{U} \in \mathbb{R}^{H \times L_M}$. At run time, with an input protein encoding $\mathbf{x}' \in \mathbb{R}^{L \times d}$, the first L columns from matrix $\mathbf{U} \in \mathbb{R}^{H \times L_M}$ can be used, which leads to: $\mathbf{s} = \mathbf{U}_{(:,1:L)} \mathbf{x}' + \mathbf{b}$, where $\mathbf{U}_{(:,1:L)}$ denotes the sub-matrix of \mathbf{U} which includes all the rows and the first L columns of \mathbf{U} . The complexity of the function described in (4) depends on the length of the protein under consideration, while the memory complexity scales linearly with the length of the longest protein. This is the same as our current approach where one model is fit to individual proteins. It differs in that the weights included up to a column l would be shared between all the proteins of length at least l . This makes the transformer learn to organize information, by placing what is relevant to all proteins in the first rows of the representation $\mathbf{x}' \in \mathbb{R}^{H \times d}$. An issue with this approach when training on DMS data is that the meaning, support and distributions of the DMS scores vary largely across DMS datasets, thus requiring the fitness scores to be standardized (Fig. A.9). An interesting future research direction is the quantification of similarities in selection assays of DMS datasets, so that they can be exploited in regression models.

5 CONCLUSION

We proposed a transformer-based matrix variational auto-encoder together with a structured prior distribution. We evaluated the performances of the model on a variant effect prediction using DMS and MSA datasets from the ProteinGym benchmark. When training on MSA data (matVAE-MSA) and performing zero-shot predictions on the DMS dataset, our proposed approach outperforms the state-of-art DeepSequence model. Our model achieves this with an order of magnitude fewer parameters, and less computations at inference time. Our architecture allowed to compare performances with models of similar capacity but trained on DMS datasets (matENC-DMS) instead of MSA. We then trained our architecture solely on DMS. DMS datasets were often much smaller than MSA data for the same protein. matENC-DMS still outperformed matVAE-MSA on average for supervised prediction tasks. We saw further increase in performances when using alphafold generated structures in our transformer model, which lead to similar performances compared to DeepSequence pretrained on MSA and finetuned on DMS data. This additionally shows the efficacy of our method. DMS assays may thus replace MSAs entirely, without major losses in performances. This in turn motivates the development of DMS datasets and the study of their relationships, in order to further improve variant effect prediction.

REFERENCES

- Ivan A. Adzhubei, Steffen Schmidt, Leonid Peshkin, Vasily E. Ramensky, Anna Gerasimova, Peer Bork, Alexey S. Kondrashov, and Shamil R. Sunyaev. A method and server for predicting damaging missense mutations. *Nature Methods*, 7(4):248–249, April 2010. ISSN 1548-7105. doi: 10.1038/nmeth0410-248.
- Jimmy Lei Ba, Jamie Ryan Kiros, and Geoffrey E. Hinton. Layer Normalization. *arXiv:1607.06450 [cs, stat]*, July 2016.
- Yinghui Chen, Yunxin Xu, Di Liu, Yaoguang Xing, and Haipeng Gong. An end-to-end framework for the prediction of protein structure and fitness from single sequence. *Nature Communications*, 15(1):7400, August 2024. ISSN 2041-1723. doi: 10.1038/s41467-024-51776-x.
- Nat Dilokthanakul, Pedro A. M. Mediano, Marta Garnelo, Matthew C. H. Lee, Hugh Salimbeni, Kai Arulkumaran, and Murray Shanahan. Deep Unsupervised Clustering with Gaussian Mixture Variational Autoencoders, January 2017.
- R Durbin. Biological sequence analysis: Probabilistic models of proteins and nucleic acids, 1998.
- Douglas M. Fowler and Stanley Fields. Deep mutational scanning: A new style of protein science. *Nature Methods*, 11(8):801–807, August 2014. ISSN 1548-7105. doi: 10.1038/nmeth.3027.
- Jonathan Frazer, Pascal Notin, Mafalda Dias, Aidan Gomez, Joseph K. Min, Kelly Brock, Yarin Gal, and Debora S. Marks. Disease variant prediction with deep generative models of evolutionary data. *Nature*, 599(7883):91–95, November 2021. ISSN 1476-4687. doi: 10.1038/s41586-021-04043-8.
- Sam Gelman, Sarah A. Fahlberg, Pete Heinzelman, Philip A. Romero, and Anthony Gitter. Neural networks to learn protein sequence–function relationships from deep mutational scanning data. *Proceedings of the National Academy of Sciences*, 118(48):e2104878118, November 2021. doi: 10.1073/pnas.2104878118.
- Kaiming He, Xiangyu Zhang, Shaoqing Ren, and Jian Sun. Identity Mappings in Deep Residual Networks. In Bastian Leibe, Jiri Matas, Nicu Sebe, and Max Welling (eds.), *Computer Vision – ECCV 2016*, pp. 630–645, Cham, 2016. Springer International Publishing. ISBN 978-3-319-46493-0. doi: 10.1007/978-3-319-46493-0_38.
- Chloe Hsu, Hunter Nisonoff, Clara Fannjiang, and Jennifer Listgarten. Learning protein fitness models from evolutionary and assay-labeled data. *Nature Biotechnology*, 40(7):1114–1122, July 2022. ISSN 1546-1696. doi: 10.1038/s41587-021-01146-5.
- Po-Ssu Huang, Scott E. Boyken, and David Baker. The coming of age of de novo protein design. *Nature*, 537(7620):320–327, September 2016. ISSN 1476-4687. doi: 10.1038/nature19946.

-
- M. Ingelman-Sundberg, S. Mkrtchian, Y. Zhou, and V.M. Lauschke. Integrating rare genetic variants into pharmacogenetic drug response predictions. *Human Genomics*, 12(1), 2018. ISSN 1473-9542. doi: 10.1186/s40246-018-0157-3.
- John Jumper, Richard Evans, Alexander Pritzel, Tim Green, Michael Figurnov, Olaf Ronneberger, Kathryn Tunyasuvunakool, Russ Bates, Augustin Žídek, Anna Potapenko, Alex Bridgland, Clemens Meyer, Simon A. A. Kohl, Andrew J. Ballard, Andrew Cowie, Bernardino Romera-Paredes, Stanislav Nikolov, Rishub Jain, Jonas Adler, Trevor Back, Stig Petersen, David Reiman, Ellen Clancy, Michal Zielinski, Martin Steinegger, Michalina Pacholska, Tamas Berghammer, Sebastian Bodenstein, David Silver, Oriol Vinyals, Andrew W. Senior, Koray Kavukcuoglu, Pushmeet Kohli, and Demis Hassabis. Highly accurate protein structure prediction with AlphaFold. *Nature*, 596(7873):583–589, August 2021. ISSN 1476-4687. doi: 10.1038/s41586-021-03819-2.
- Diederik P. Kingma and Max Welling. Auto-Encoding Variational Bayes. *arXiv:1312.6114 [cs, stat]*, May 2014.
- Elodie Laine, Yasaman Karami, and Alessandra Carbone. GEMME: A Simple and Fast Global Epistatic Model Predicting Mutational Effects. *Molecular Biology and Evolution*, 36(11):2604–2619, November 2019. ISSN 0737-4038. doi: 10.1093/molbev/msz179.
- Céline Marquet, Michael Heinzinger, Tobias Olenyi, Christian Dallago, Kyra Erckert, Michael Bernhofer, Dmitrii Nechaev, and Burkhard Rost. Embeddings from protein language models predict conservation and variant effects. *Human Genetics*, 141(10):1629–1647, October 2022. ISSN 1432-1203. doi: 10.1007/s00439-021-02411-y.
- Pauline C. Ng and Steven Henikoff. SIFT: Predicting amino acid changes that affect protein function. *Nucleic Acids Research*, 31(13):3812–3814, July 2003. ISSN 0305-1048. doi: 10.1093/nar/gkg509.
- Pascal Notin, Mafalda Dias, Jonathan Frazer, Javier Marchena Hurtado, Aidan N. Gomez, Debora Marks, and Yarin Gal. Tranception: Protein Fitness Prediction with Autoregressive Transformers and Inference-time Retrieval. In *Proceedings of the 39th International Conference on Machine Learning*, pp. 16990–17017. PMLR, June 2022a.
- Pascal Notin, Lood Van Niekerk, Aaron W. Kollasch, Daniel Ritter, Yarin Gal, and Debora S. Marks. TranceptEVE: Combining Family-specific and Family-agnostic Models of Protein Sequences for Improved Fitness Prediction, December 2022b.
- Pascal Notin, Aaron W. Kollasch, Daniel Ritter, Lood Van Niekerk, Steffan Paul, Han Spinner, Nathan J. Rollins, Ada Shaw, Rose Orenbuch, Ruben Weitzman, Jonathan Frazer, Mafalda Dias, Dinko Franceschi, Yarin Gal, and Debora Susan Marks. ProteinGym: Large-Scale Benchmarks for Protein Fitness Prediction and Design. In *Thirty-Seventh Conference on Neural Information Processing Systems Datasets and Benchmarks Track*, November 2023a.
- Pascal Notin, Ruben Weitzman, Debora Marks, and Yarin Gal. Proteinnpt: Improving protein property prediction and design with non-parametric transformers. *Advances in Neural Information Processing Systems*, 36:33529–33563, 2023b.
- Andres Potapczynski, Gabriel Loaiza-Ganem, and John P. Cunningham. Invertible Gaussian Reparameterization: Revisiting the Gumbel-Softmax, October 2020.
- Roshan M. Rao, Jason Liu, Robert Verkuil, Joshua Meier, John Canny, Pieter Abbeel, Tom Sercu, and Alexander Rives. MSA Transformer. In *Proceedings of the 38th International Conference on Machine Learning*, pp. 8844–8856. PMLR, July 2021.
- Adam J. Riesselman, John B. Ingraham, and Debora S. Marks. Deep generative models of genetic variation capture the effects of mutations. *Nature Methods*, 15(10):816–822, October 2018. ISSN 1548-7105. doi: 10.1038/s41592-018-0138-4.
- Alexander Rives, Joshua Meier, Tom Sercu, Siddharth Goyal, Zeming Lin, Jason Liu, Demi Guo, Myle Ott, C. Lawrence Zitnick, Jerry Ma, and Rob Fergus. Biological structure and function emerge from scaling unsupervised learning to 250 million protein sequences. *Proceedings of the National Academy of Sciences*, 118(15):e2016239118, April 2021. doi: 10.1073/pnas.2016239118.

Jakub M. Tomczak and Max Welling. VAE with a VampPrior, February 2018.

Yasemin Bozkurt Varolgüneş, Tristan Berreau, and Joseph F. Rudzinski. Interpretable embeddings from molecular simulations using Gaussian mixture variational autoencoders. *Machine Learning: Science and Technology*, 1(1):015012, April 2020. ISSN 2632-2153. doi: 10.1088/2632-2153/ab80b7.

Ashish Vaswani, Noam Shazeer, Niki Parmar, Jakob Uszkoreit, Llion Jones, Aidan N. Gomez, Lukasz Kaiser, and Illia Polosukhin. Attention Is All You Need, December 2017.

Kevin K Yang, Niccolò Zanichelli, and Hugh Yeh. Masked inverse folding with sequence transfer for protein representation learning. *Protein Engineering, Design and Selection*, 36:gza015, January 2023. ISSN 1741-0126. doi: 10.1093/protein/gza015.

Yitian Zhou, Roman Tremmel, Elke Schaeffeler, Matthias Schwab, and Volker M. Lauschke. Challenges and opportunities associated with rare-variant pharmacogenomics. *Trends in Pharmacological Sciences*, 43(10):852–865, October 2022. ISSN 01656147. doi: 10.1016/j.tips.2022.07.002.

A APPENDIX

A.1 ENTROPY MINIMIZATION OF DISCRETE LATENT VECTORS

Let $d \in \mathbb{N}$, and $\forall i \in [d] \ \alpha_i > 0$. Suppose $\alpha = (\alpha_1, \dots, \alpha_d)$ is the parameter vector of a Dirichlet distribution with d categories. Let $X \sim \text{Dir}(\alpha)$. Let Z a one-of- d binary vector such that $\forall i \in [d] \ \mathbb{P}(Z_i = 1, Z_{j \neq i} = 0) = X_i$. We have the conditional entropy:

$$H(Z|X) = \mathbb{E}[-\ln \mathbb{P}(Z|X)] = -\sum_{i=1}^d X_i \ln X_i. \quad (8)$$

Let \mathbb{P}_U denote a discrete uniform distribution with a support of size d . We also have that

$$H(Z|X) = \ln d - \mathbb{E}_X [D_{KL}(\mathbb{P}(Z|X) || \mathbb{P}_U(Z))]. \quad (9)$$

Proof. By definition (Cover & Thomas) we have: $H(Z|X) = H(Z) - I(Z; X)$. To prove Eq. (9), the idea is to introduce the uniform discrete distribution in the terms on the RHS:

$$H(Z) = -\sum_i \mathbb{P}(Z_i) \ln \mathbb{P}(Z_i) \quad (10)$$

$$= -\sum_i \mathbb{P}(Z_i) \ln \frac{\mathbb{P}(Z_i) \mathbb{P}_U(Z_i)}{\mathbb{P}_U(Z_i)} \quad (11)$$

$$= -\sum_i \mathbb{P}(Z_i) \ln \mathbb{P}_U(Z_i) - \sum_i \mathbb{P}(Z_i) \ln \frac{\mathbb{P}(Z_i)}{\mathbb{P}_U(Z_i)} \quad (12)$$

$$= \ln d - D_{KL}(\mathbb{P}(Z) || \mathbb{P}_U(Z)) \quad (13)$$

Similarly, we introduce the uniform discrete distribution in the mutual information:

$$I(Z; X) = D_{KL}(\mathbb{P}(Z, X) || \mathbb{P}(Z)\mathbb{P}(X)) \quad (14)$$

$$= \sum_{z,x} \mathbb{P}(z, x) \ln \frac{\mathbb{P}(z, x)}{\mathbb{P}(z)\mathbb{P}(x)} \quad (15)$$

$$= \sum_{z,x} \mathbb{P}(z, x) \ln \frac{\mathbb{P}(z, x) \mathbb{P}_U(z)}{\mathbb{P}(z)\mathbb{P}(x)\mathbb{P}_U(z)} \quad (16)$$

$$= \sum_{z,x} \mathbb{P}(z, x) \ln \left[\frac{\mathbb{P}(z, x)}{\mathbb{P}(x)\mathbb{P}_U(z)} + \frac{\mathbb{P}_U(z)}{\mathbb{P}(z)} \right] \quad (17)$$

$$= D_{KL}(\mathbb{P}(Z, X) || \mathbb{P}_U(Z)\mathbb{P}(X)) - \sum_z \ln \frac{\mathbb{P}(z)}{\mathbb{P}_U(z)} \sum_x \mathbb{P}(z, x) \quad (18)$$

$$= \mathbb{E}_X [D_{KL}(\mathbb{P}(Z|X) || \mathbb{P}_U(Z))] - D_{KL}(\mathbb{P}(Z) || \mathbb{P}_U(Z)) \quad (19)$$

Subtracting the terms concludes the proof:

$$H(Z|X) = \ln d - \mathbb{E}_X [D_{KL}(\mathbb{P}(Z|X) || \mathbb{P}_U(Z))] \quad (20)$$

□

Therefore decreasing $H(Z|X)$ increases $\mathbb{E}_X [D_{KL}(\mathbb{P}(Z|X) || \mathbb{P}_U(Z))]$, i.e. in the limit,

$$H(Z|X) \rightarrow 0 \implies \mathbb{P}(Z|X) \rightarrow Q(Z) \quad (21)$$

where $Q(Z)$ is the one-of- d discrete distribution with entropy $H(Q) = 0$.

A.2 DATASETS

We train separate models on 26 pharmacogene-related proteins for which the DMS and MSA datasets are readily available from the publicly available ProteinGym repository (Notin et al., 2023a). The pharmacogene-related proteins were divided into four functional categories: Drug Targets ($n = 21$) and Absorption-Distribution-Metabolism-Excretion (ADME) related proteins ($n = 5$). The ADME category is further divided into Cytochrome (“CYP”), “transporter” and “other” ADME proteins. In total we compare performances on 33 DMS datasets, some proteins having several DMS datasets obtained under different selection assays (Table A.4).

A.2.1 PREPROCESSING OF MSA SEQUENCES

We followed the preprocessing steps proposed in DeepSequence for the MSA data (Riesselman et al., 2018). Sequences are removed from MSAs if they include more than 50% gaps. Columns are removed from a MSA if they contain more than 30% gaps across the MSA. For consistency, the columns that are removed from the MSA are also removed from the DMS datasets of that protein. When training on MSAs, each sequence is sampled with a probability proportional to the reciprocal of the number of sequences within a given Hamming distance from that sequence (Riesselman et al., 2018). A summary description of the datasets is provided in Table A.3.

Table A.3: Description of DMS and MSA datasets per protein category. The most extreme values are in bold. L: Preprocessed sequence length; MSA Num Seq (resp. DMS Num Seq): number of sequences in the MSA (resp. DMS) datasets. ADME trans.: ADME Transporter.

Category		L	MSA Num Seq	DMS Num Seq
ADME CYP (n=2)	$\mu \pm \sigma$	490 \pm 0	260849 \pm 0	6256 \pm 161
	min/max	490 / 490	260849 / 260849	6142 / 6370
ADME other (n=2)	$\mu \pm \sigma$	204 \pm 57	86361 \pm 94716	3246 \pm 569
	min/max	164 / 245	19387 / 153335	2844 / 3648
ADME tran. (n=3)	$\mu \pm \sigma$	579 \pm 44	144978 \pm 90553	10491 \pm 951
	min/max	553 / 630	40416 / 197259	9803 / 11576
Drug target (n=26)	$\mu \pm \sigma$	498 \pm 427	62331 \pm 125352	3374 \pm 3134
	min/max	31 / 1863	911 / 611225	63 / 12464

A.3 MODEL ARCHITECTURES HYPER-PARAMETERS

The encoding and decoding transformers of matVAE-MSA are designed with 3 transformer layers described in (3). The embedding dimensions of all the layers are identical and equal to d . The use of 3 layers allows to use information from neighbors up to order 3 according to the graph defined by the attention mask. The attention mask is a thresholded distance matrix derived from the WT protein structures predicted by Alphafold2 (Jumper et al., 2021). This means that queries are allowed to attend to keys in the attention dot product if the predicted distance in 3d between the corresponding AAs is $\leq c$. We chose $c = 7\text{\AA}$ which had the best performances for 4 out of 5 graph neural network-based models predicting variant effects in (Gelman et al., 2021, Table S3). The structures are readily available in the ProteinGym repository as PDB files (Notin et al., 2023a). For DwFC, we chose $H = \min(H_{min}, L)$ with $H_{min} = 200$. This means that the dimension is not reduced for proteins with small enough sequence length $L \leq H_{min}$. Following the discussion in Section 2.1.1, we experimented with $H_{min} \approx d$ on some proteins, but could not get good performances. For FCB, we used a 2-layer ReLU network with 1000 and 300 neurons, and output latent space dimension $D = 10$, this is smaller than the design of DeepSequence which uses $D = 50$ (Riesselman et al., 2018). Symmetrical design choices were used for the decoding part of matVAE-MSA. For training, we use $\beta = 0.01$ and at test time (i.e. when computing the ELBO) we use $\beta = 1$. We found that larger β caused the latent vectors to collapse to identical vectors, and smaller β caused the training to be unconstrained, i.e. leading to uniform vectors. For matENC-DMS, the D -dimensional latent vector in the FC bottleneck is passed into a prediction head with a 1-layer fully connected ReLU network, with 10 neurons, and an output dimension of 1. The decoding parts of matVAE-MSA are not used.

A.4 MODEL TRAINING

For matVAE-MSA, the models are trained on protein specific MSAs to minimize the negative ELBO in (6). The expected reconstruction error is approximated with a 1-sample Monte Carlo method. The reconstruction error is the cross-entropy between the true $\mathbf{x} \in \mathbb{R}^{L \times d}$ and the reconstructed $\hat{\mathbf{x}}$. For matENC-DMS, no variational formulation is used. The loss function is the mean squared error (MSE) between the true label $y \in \mathbb{R}$ and the reconstructed label \hat{y} .

For all our included proteins, the loss function for matVAE-MSA is optimized using the ADAM optimizer, with a fixed learning rate $\lambda = 8e - 5$, a batch size of 256 and 300,000 training steps. For matENC-DMS, the loss function is optimized with a fixed learning rate $\lambda = 1e - 4$, a batch size of 512 and 100,000 training steps. The learning rates were chosen similar to the optimal one reported

for a graph neural network model in (Gelman et al., 2021, Table S3). The batch sizes were chosen to obtain the most efficient use of our hardware. In matVAE-MSA, the memory footprint is mainly due to the attention matrices in the encoder and decoder transformer. We double the batch size for matENC-DMS compared to matVAE-MSA since matENC-DMS only has an encoder transformer.

A.5 RAW SPEARMANR AND AUROC PERFORMANCES FOR ZERO-SHOT LEARNING TASKS

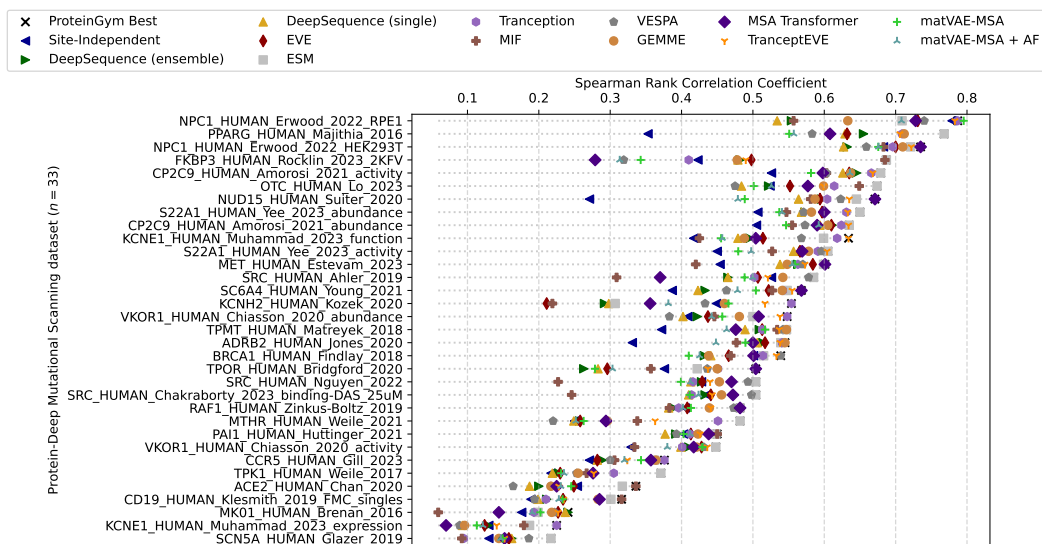


Figure A.4: Raw Spearman Rank correlation coefficient performances on all DMS datasets for zero-shot prediction task. We display the performances of our models against the best performing models in ProteinGym for pharmacogene-related proteins. The datasets are sorted in decreasing “best benchmark” performances.

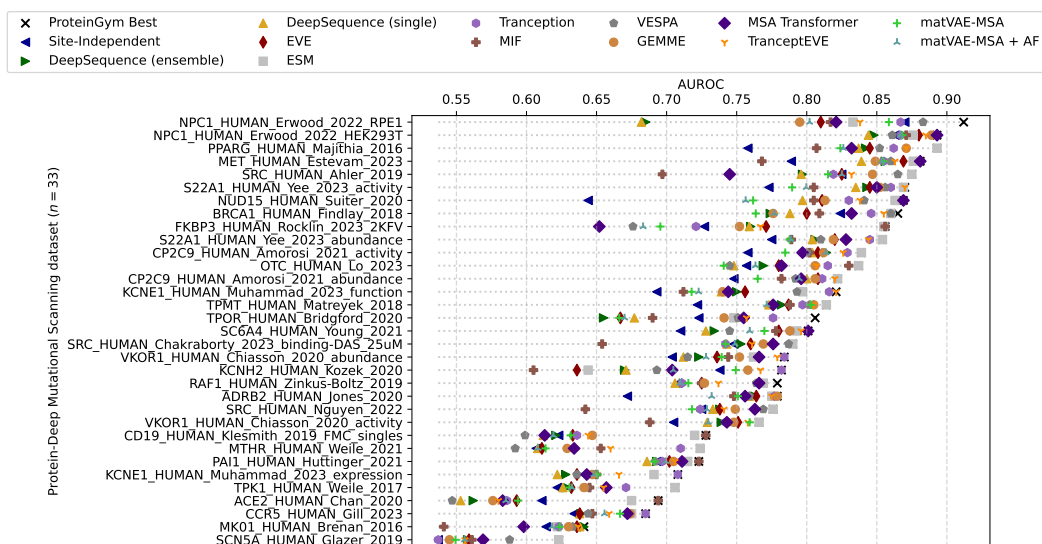


Figure A.5: AUROC performances on all DMS datasets for zero-shot prediction task. We display the performances of our models against the best performing models in ProteinGym for pharmacogene-related proteins. The datasets are sorted in decreasing “best benchmark” performances.

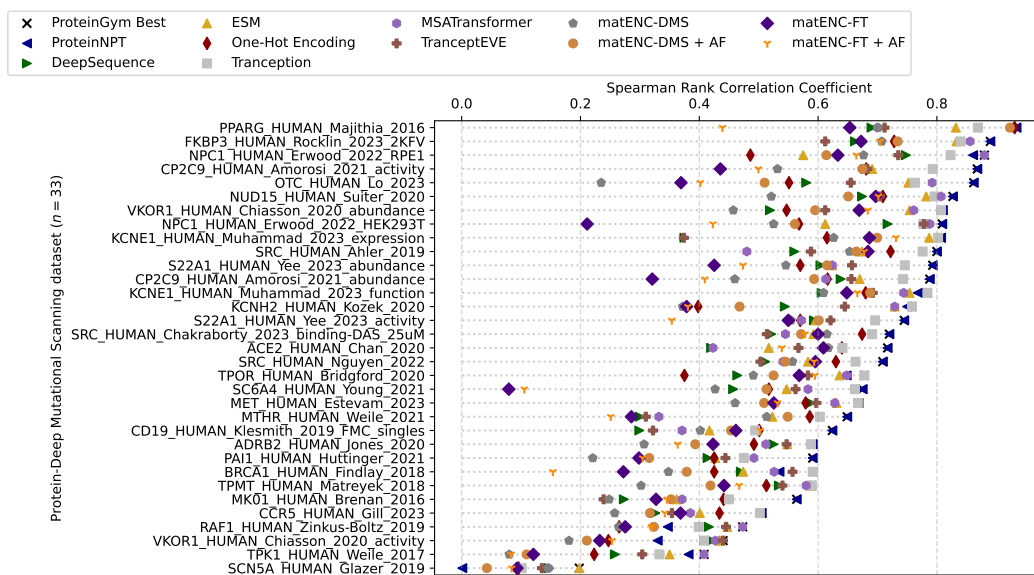


Figure A.6: SpearmanR performances on all DMS datasets for a supervised learning task. We display the performances of our models against the best performing models in ProteinGym for pharmacogene-related proteins. The datasets are sorted in decreasing “best benchmark” performances.

A.6 PERFORMANCES ACCORDING TO PROTEIN CATEGORY

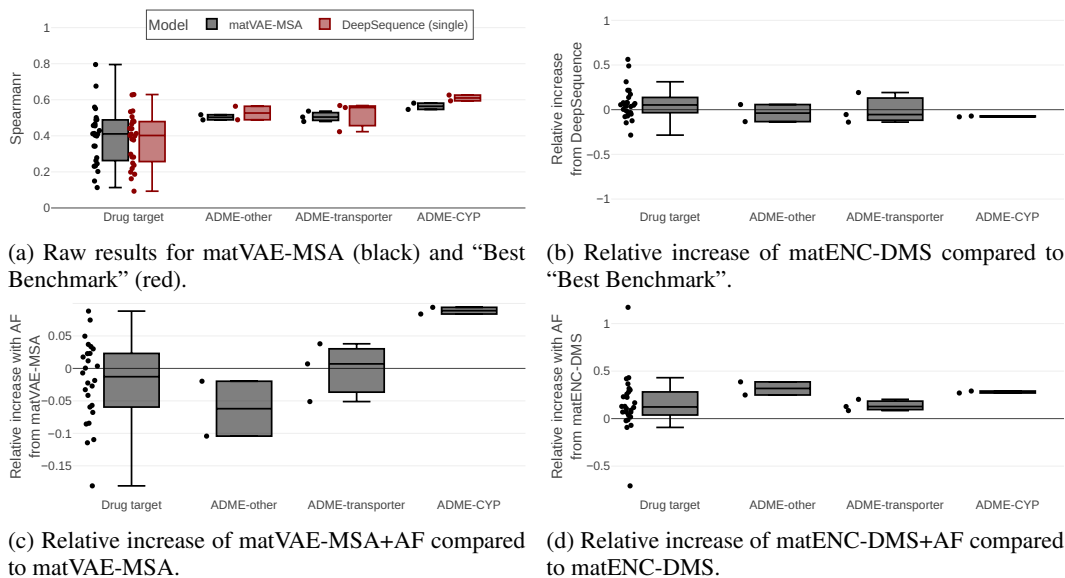


Figure A.7: SpearmanR performances of matENC-DMS versus other zero-shot prediction models, per protein category. One point denotes the score obtained on a DMS dataset and the boxplots describe the distribution of scores across DMS datasets.

A.7 STUDYING POSSIBLE CONFOUNDER FOR RELATIVE INCREASE OF FINETUNING FROM MSA

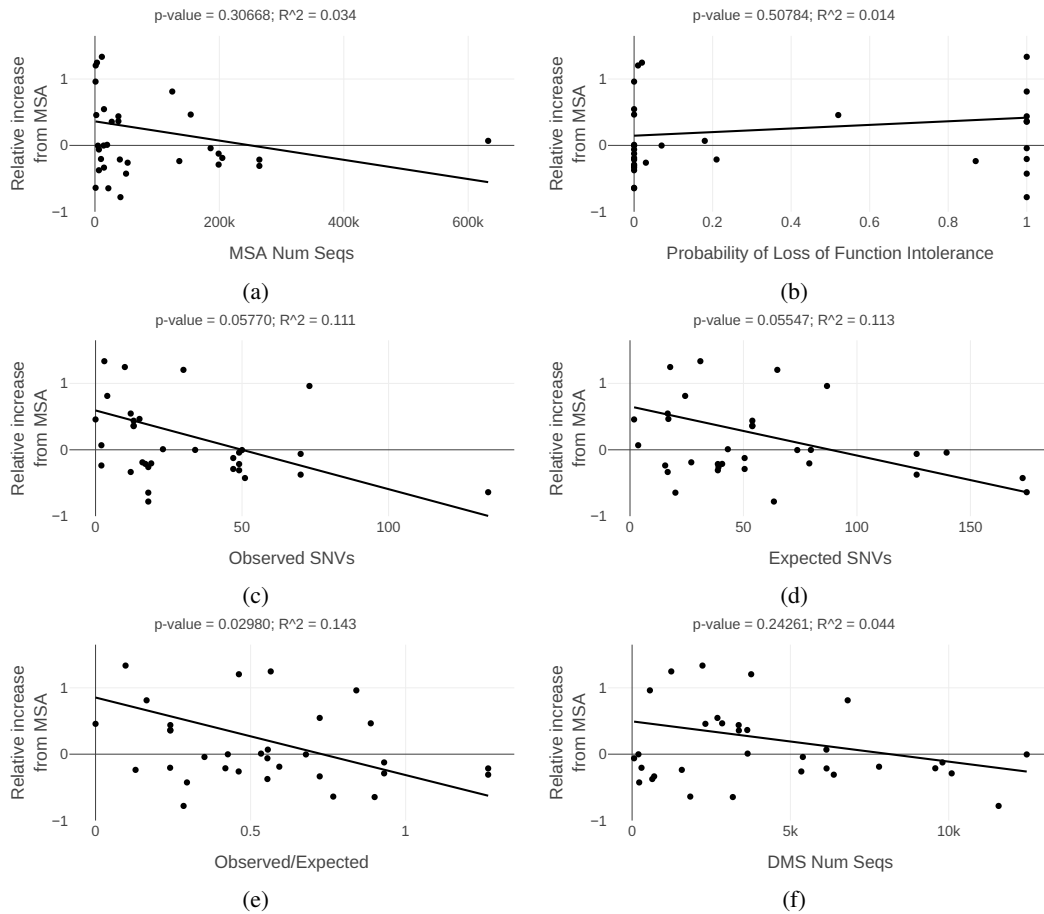


Figure A.8: Univariate correlation analysis for potential confounders of the relative increase of matENC-DMS + AF from matVAE-MSA + AF. None of the considered confounders are significant to explain the relative increase from MSA. A multivariate correlation analysis was performed and did not show any significance (not shown). **MSA Num Seqs**: Number of variants in MSA; **Probability of Loss of Function Intolerance**: Genes with a pLI close to 1 are often associated with haploinsufficiency and dominant genetic diseases; **Expected (resp. Observed) SNVs**: Expected (resp. Observed) Single-nucleotide variant in each gene; **Observed/Expected (o/e)**: Constrained genes have fewer observed variants than expected (low o/e) and are under a higher degree of selection than less constrained genes. **DMS Num Seqs**: Number of variants in DMS data;

A.8 ADDITIONAL DATASET INFORMATION

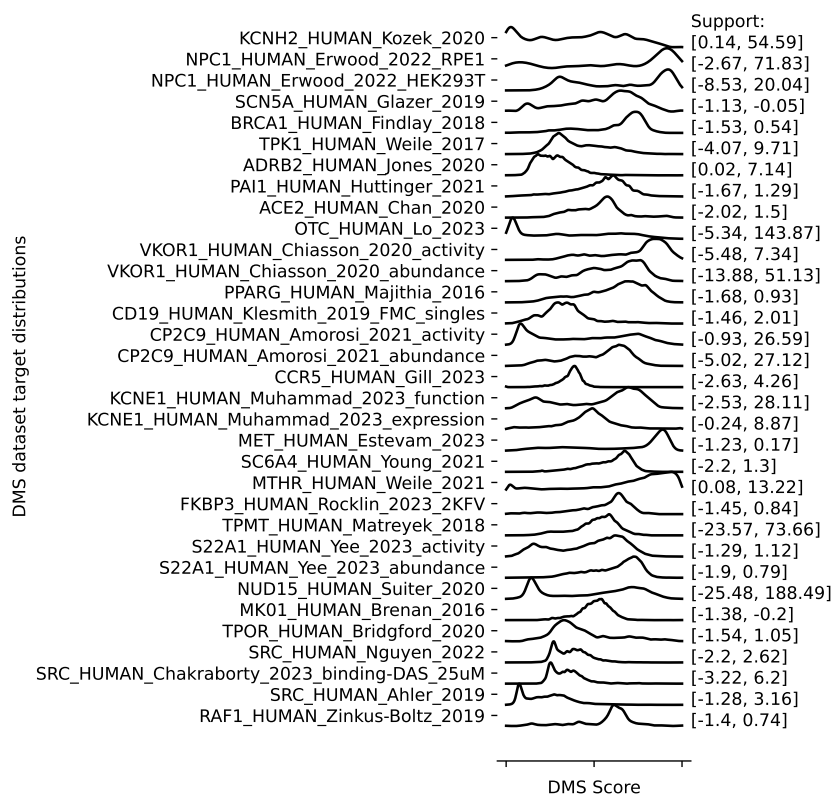


Figure A.9: Empirical kernel density estimates of the density function of DMS datasets target score. The support and range of each density function are standardized to $[0,1]$ for visualization. The true support of the density functions is annotated on the right hand side. The densities are displayed with an increment of 1 along the y-axis.

Category	UniProt ID	L	MSA Num Seq	DMS Num Seq	Selection Type	Best Benchmark - Flavor
ADME CYP	CP2C9	490	260849	6142	Binding	ESM2 (150M)
				6370	Expression	ESM2 (650M)
ADME other	NUD15	164	153335	2844	Expression	MSA Transformer (ensemble)
	TPMT	245	19387	3648	Expression	ESM-1v (ensemble)
ADME transporter	S22A1	553	197259	9803	Expression	ESM-1v (ensemble)
	SC6A4	630	40416	10094 11576	Activity Activity	ESM-1v (ensemble) MSA Transformer (ensemble)
Drug target	ACE2	805	10865	2223	Binding	MIF
	ADRB2	413	201108	7800	Activity	GEMME
	BRCA1	1863	974	1837	Organismal	VESPA
					Fitness	
	CCR5	352	611225	6137	Binding	Tranception L
	CD19	556	1171	3761	Binding	MIF
	FKBP3	69	3211	1237	Stability	ESM-IF1
	KCNE1	129	2104	2315	Activity	TranceptEVE L
					Expression	Tranception M no retrieval
	KCNH2	31	13900	200	Activity	Tranception M
	MET	287	184827	5393	Activity	MSA Transformer (ensemble)
	MK01	360	123422	6809	Organismal	DeepSequence (ensemble)
					Fitness	
	MTHR	656	4724	12464	Organismal	ESM2 (150M)
	NPC1	1278	6234	63	Fitness	
					Activity	Tranception S
	OTC	354	134484	1570	Activity	MSA Transformer (ensemble)
					Activity	ESM-IF1
	PAI1	402	51792	5345	Activity	MIF-ST
	PPARG	505	39639	9576	Activity	ESM2 (15B)
RAF1	648	9609	297	Organismal	MSA Transformer (single)	
				Fitness		
SCN5A	32	49959	224	Organismal	ESM-1v (single)	
				Fitness		
SRC	536	37311	3366	Organismal	ESM-1v (ensemble)	
				Fitness		
TPK1	243	21338	3181	Activity	ESM-1v (ensemble)	
				Activity	ESM-1v (ensemble)	
TPOR	635	911	562	Organismal	ESM2 (15B)	
				Fitness		
VKOR1	163	14425	697	Activity	ESM-1v (ensemble)	
				Expression	Tranception L	

Table A.4: Deep Mutation Scanning datasets details retrieved from ProteinGym. **UniProt ID**: Universal protein identifier; **L**: Preprocessed sequence length; **MSA Num Seq** (resp. **DMS Num Seq**): number of sequences in the MSA (resp. DMS) datasets. **Selection Type**: DMS assay selection type. **Best Benchmark - Flavor**: best performing model flavor for zero-shot prediction tasks.

Best Benchmark - Family	Best Benchmark - Flavor
ESM (n=15)	ESM2 (15B) x2 ESM-1v (ensemble) x7 ESM2 (150M) x2 ESM2 (650M) x1 ESM-IF1 x2 ESM-1v (single) x1
MSA Transformer (n=6)	MSA Transformer (single) x2 MSA Transformer (ensemble) x4
Tranception (n=5)	Tranception L x2 Tranception S x1 Tranception M x1 Tranception M no retrieval x1
MIF (n=3)	MIF-ST x1 MIF x2
DeepSequence (n=1)	DeepSequence (ensemble) x1
TranceptEVE (n=1)	TranceptEVE L x1
GEMME (n=1)	GEMME x1
VESPA (n=1)	VESPA x1

Table A.5: Summary of best model flavors and families for zero-shot prediction tasks.

Model Family	Best Benchmark Name
ProteinNPT (n=23)	ProteinNPT x23
Tranception (n=5)	Tranception Embeddings x5
MSA Transformer (n=2)	MSA Transformer Embeddings x2
ESM (n=1)	ESM-1v + One-Hot Encodings x1
MSA Transformer + One-Hot Encodings (n=1)	MSA Transformer + One-Hot Encodings x1
TranceptEVE (n=1)	TranceptEVE + One-Hot Encodings x1

Table A.6: Summary of best model flavors and families for supervised prediction tasks.